Searching DM (WIMP and ALP) from gamma ray observations

LEI FENG （冯磊）

PURPLE MOUNTAIN OBSERVATORY

2018-10-18@ACADEMIA SINICA

COLLABORATORS： CUN ZHANG, ZI-QING XIA, YUN-FENG LIANG, SHANG LI, XIANG LI, BEI ZHOU, XIAO-YUAN HUANG,NENG-HUI LIAO, QIANG YUAN, YI-ZHONG FAN, ZHONG-ZHOU REN, JIAN WU

OUTLINE

- What is Axion and ALP？
- Dark matter and WIMP searching in gamma ray data
- Searching ALP in gamma ray data and Our works

OUTLINE

- What is Axion and ALP？
- Dark matter and DM searching in gamma ray data
- Searching ALP in gamma ray data and Our works

STRONG CP PROBLEM

1 Why Axions?

Before 1975, QCD was described by the Lagrangian

$$\mathcal{L} = -\frac{1}{2g^2}\mathrm{Tr}F_{\mu\nu}F^{\mu\nu} + \bar{q}(i\gamma^\mu D_\mu - M_q)q.$$

But after 1975, the following θ term is known to be present due to the discovery of instanton solutions in nonabelian gauge theories [1,2]

$$\frac{\bar{\theta}}{16\pi^2}\ \mathrm{Tr}F_{\mu\nu}\tilde{F}^{\mu\nu} \quad (1)$$

where $\bar{\theta} = \theta_{\mathrm{QCD}} + \theta_{\mathrm{QFD}}$ which violates CP. From the experimental bound on the neutron electric dipole moment [3], $|\bar{\theta}|$ is required to be less than 10^{-9}. This is "the strong CP problem".

WHAT IS AXION?

The axion solution of the strong CP problem is to introduce a dynamical field axion (a) so that $\bar{\theta}$ is settled very near 0.[4] In this case, one can study the following Lagrangian below the electroweak scale, after integrating out the quark fields,

$$\mathcal{L} = -\frac{1}{4g^2} F^a_{\mu\nu} F^{a\mu\nu} + \bar{q}(i\gamma^\mu D_\mu - M_q)q + \frac{a}{32\pi^2 F_a} F^a_{\mu\nu} \tilde{F}^{a\mu\nu} + \frac{1}{2}\partial^\mu a \partial_\mu a. \quad (2)$$

Here, $\bar{\theta}$ turns out to be $\bar{\theta} = a/F_a$ where F_a is called the axion decay constant. In this model, $\bar{\theta}$ is a dynamical field. But, for a moment consider $\bar{\theta}$ as a

decay constant and mass of the pion. Using $z = m_u/m_d$,

$$m_a = \frac{\sqrt{z}}{1+z}\left(\frac{f_\pi m_\pi}{f_a/N}\right) \quad (10)$$

$$= 0.60\ \text{meV}\ \frac{2\sqrt{z/0.56}}{1+(z/0.56)}\left(\frac{10^{10}\ \text{GeV}}{f_a/N}\right) . \quad (11)$$

This relation is shown for $z = 0.56$ [101] and $f_a/N \to f_a$ in Fig. 1 (from [24]); note that z could be within 0.3–0.6 [2].

OUTLINE

- What is Axion and ALP？
- Dark matter and WIMP searching in gamma ray data
- Searching ALP in gamma ray data and Our works

DARK MATTER

- Ordinary matter (4.9%)
- **Dark matter (26.8%)**
- Dark energy (68.3%)

Gravitational Lensing

CMB Power Spectrum

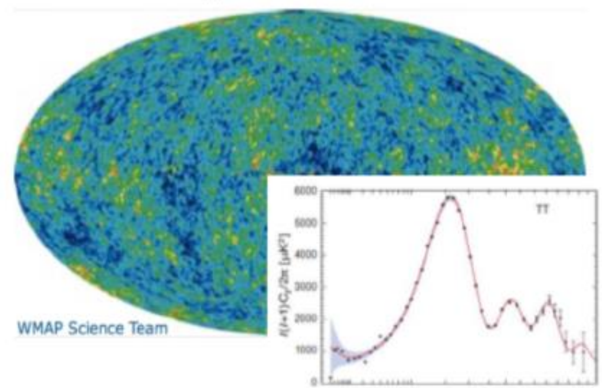

Kinematics of Galaxies and Galaxy Clusters

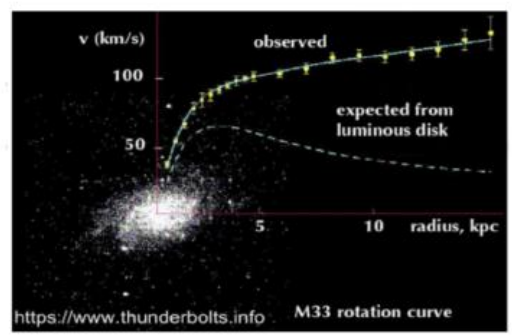

DARK MATTER CANDIDATES

- WIMPs
- **Axion/ALP**
- Sterile Neutrino
- Gravitino

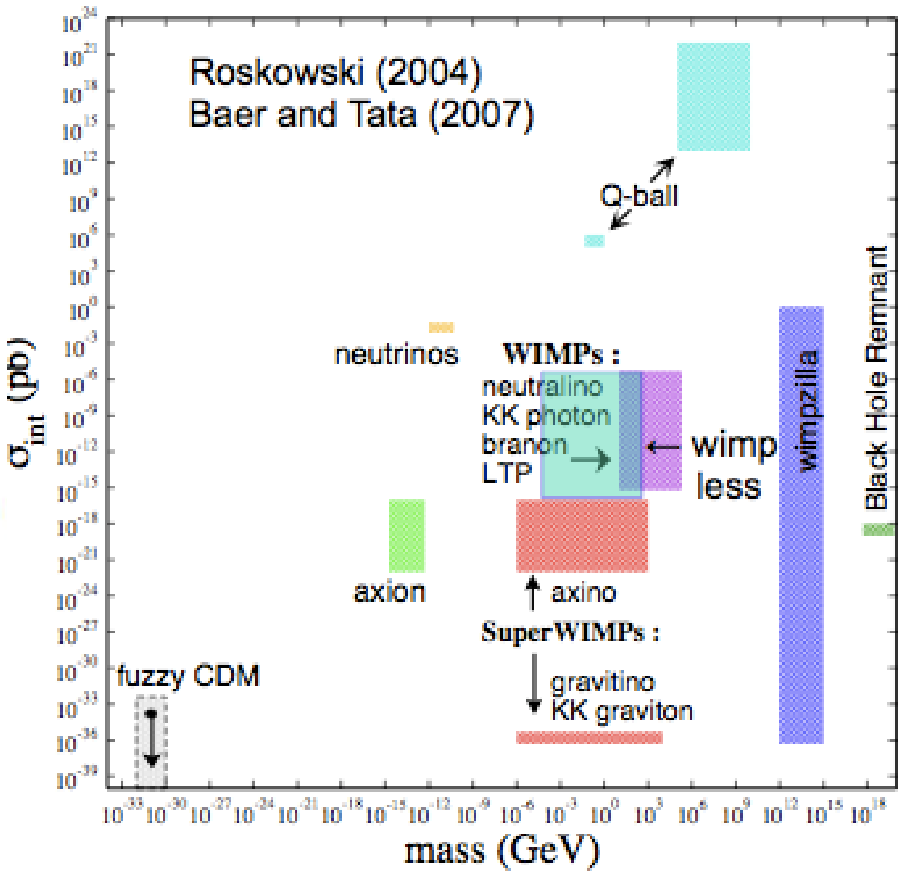

Many candidates with mass and cross section spanning many orders of magnitude

Fermi gamma-rays can provide good test of the DM models

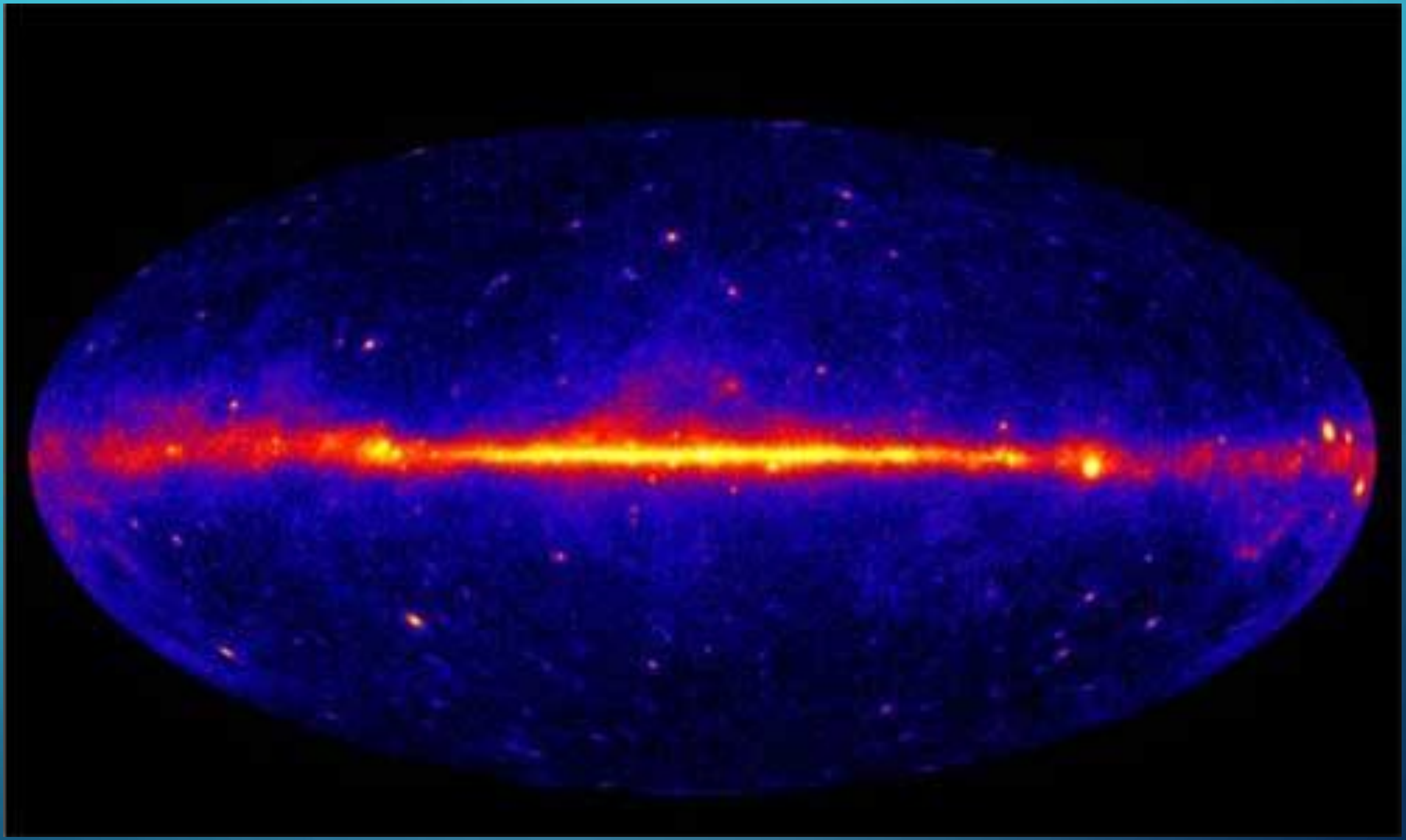

- Galactic center
- Galactic halo
- Dwarf galaxies
- Clusters
- Extra-galactic diffuse
- Line search

The signal depends on the DM annihilation channel

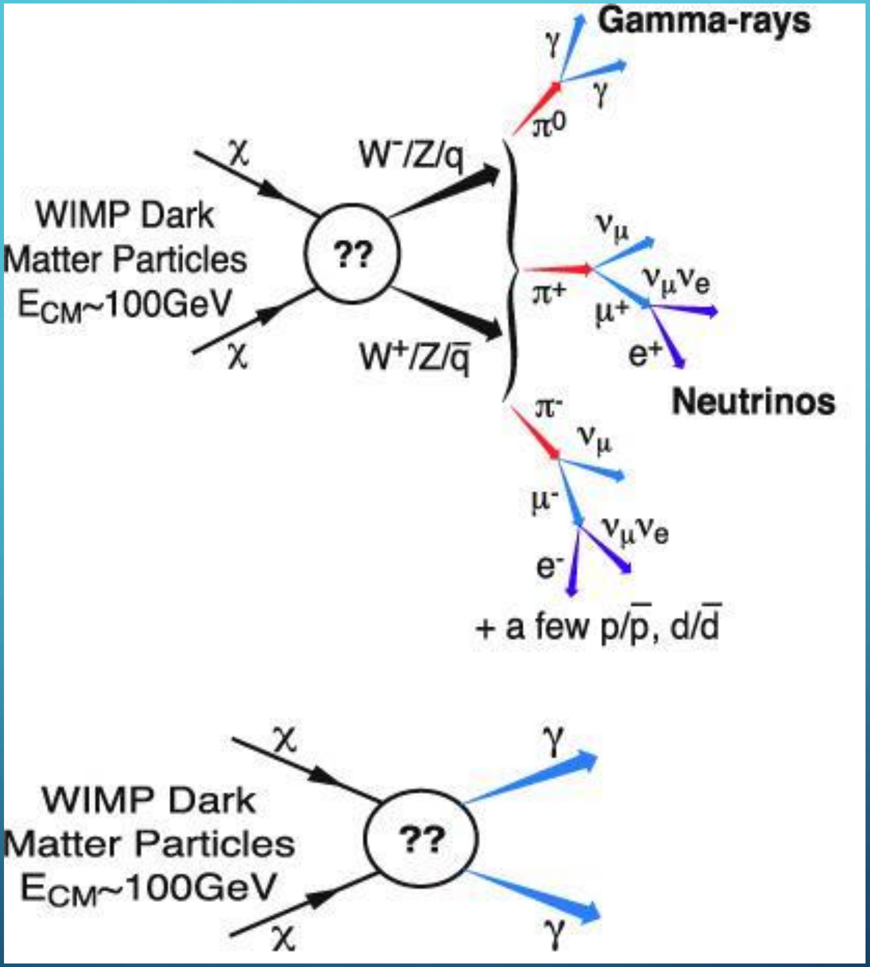

Baltz et al. 2008

THE GAMMA-RAY SKY MAP PRODUCED BY DARK MATTER ANNIHILATION IN OUR GALAXY

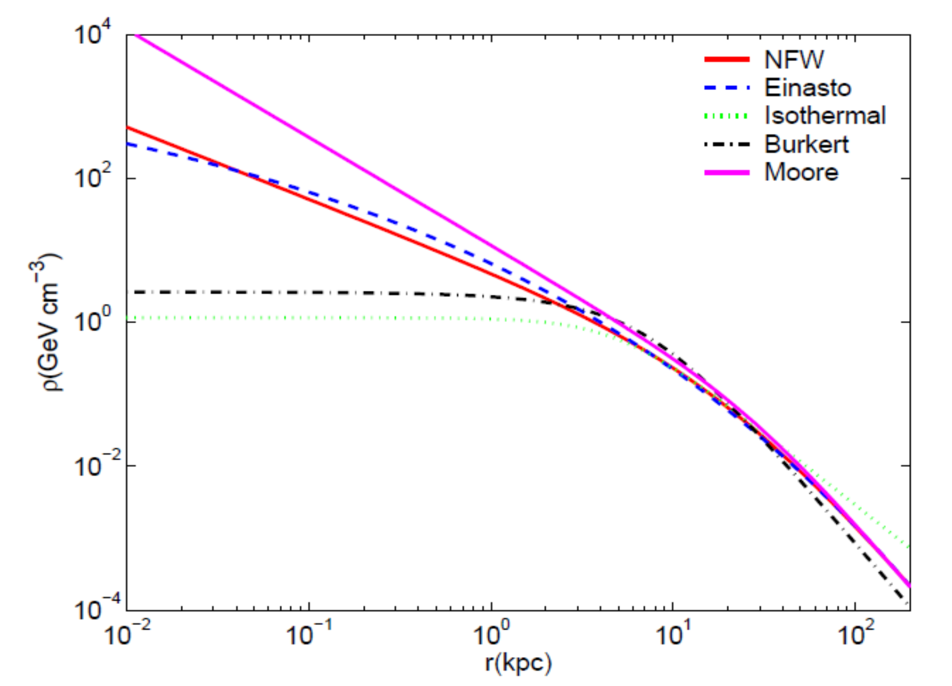

The J-Factor of different dark matter profile models.

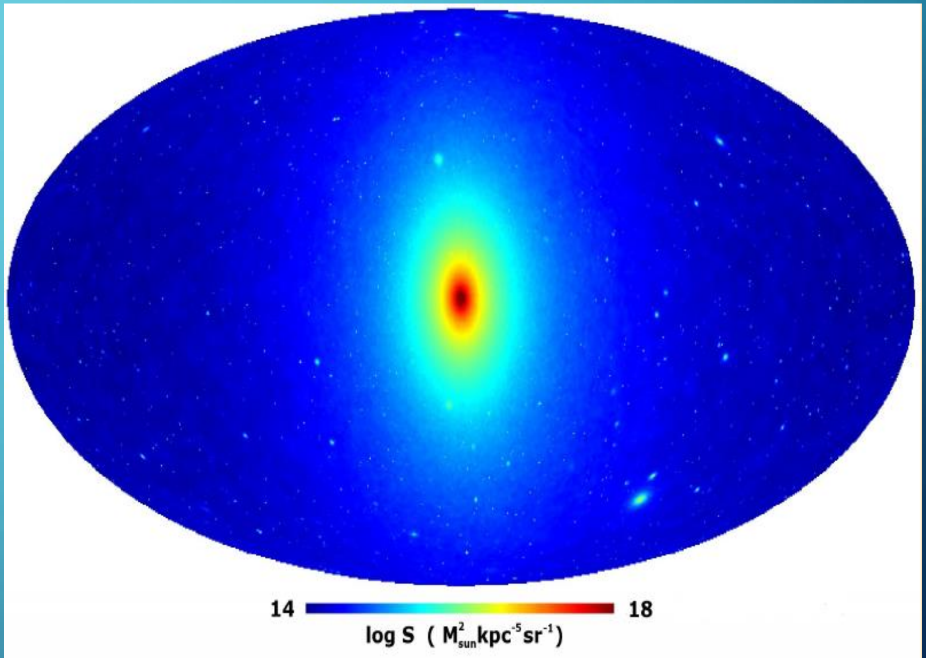

The Galaxy center is the best region to detect dark matter.

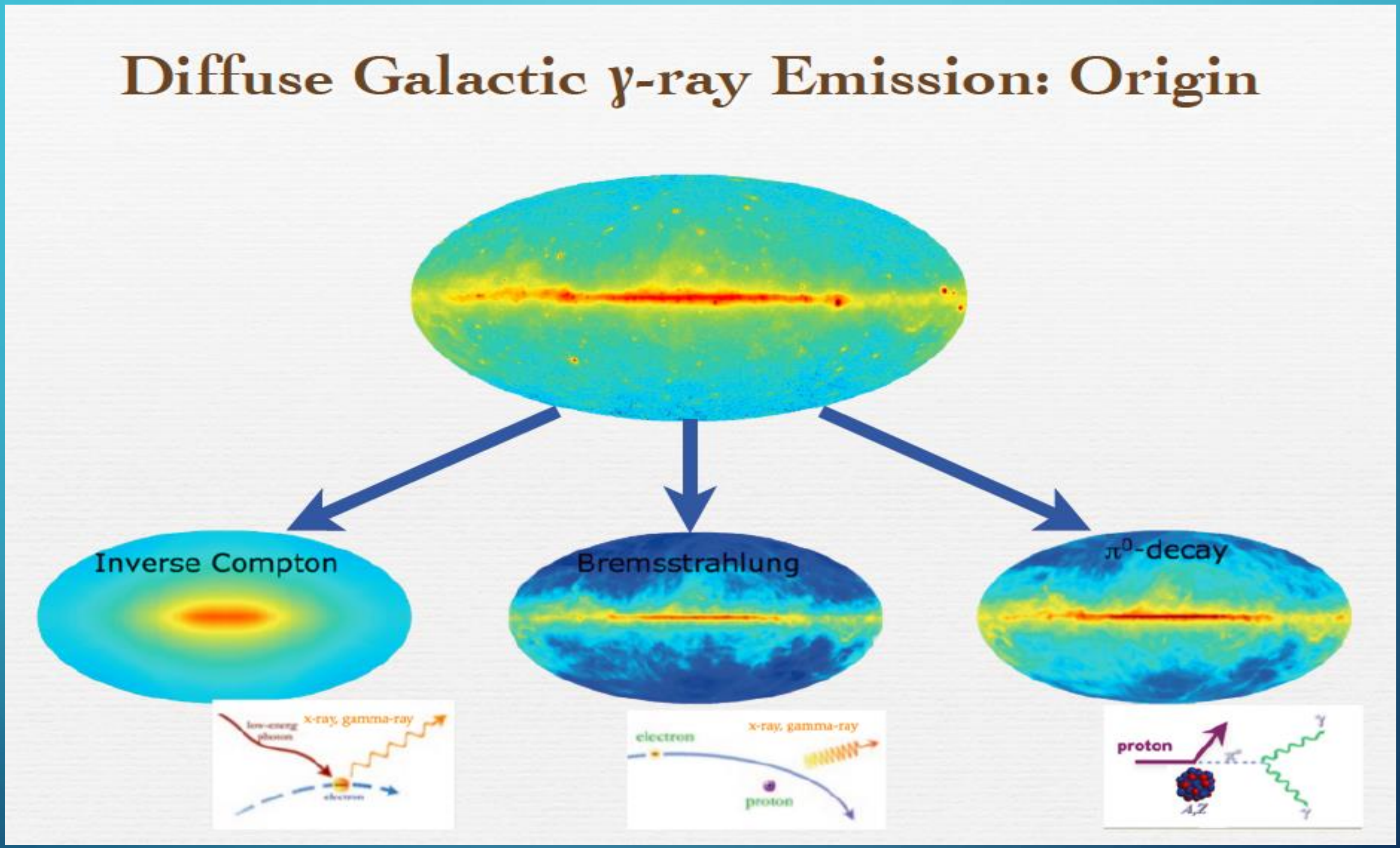

Subtract the Known components and the Residual part might be the signal of DM

THE GEV EXCESS

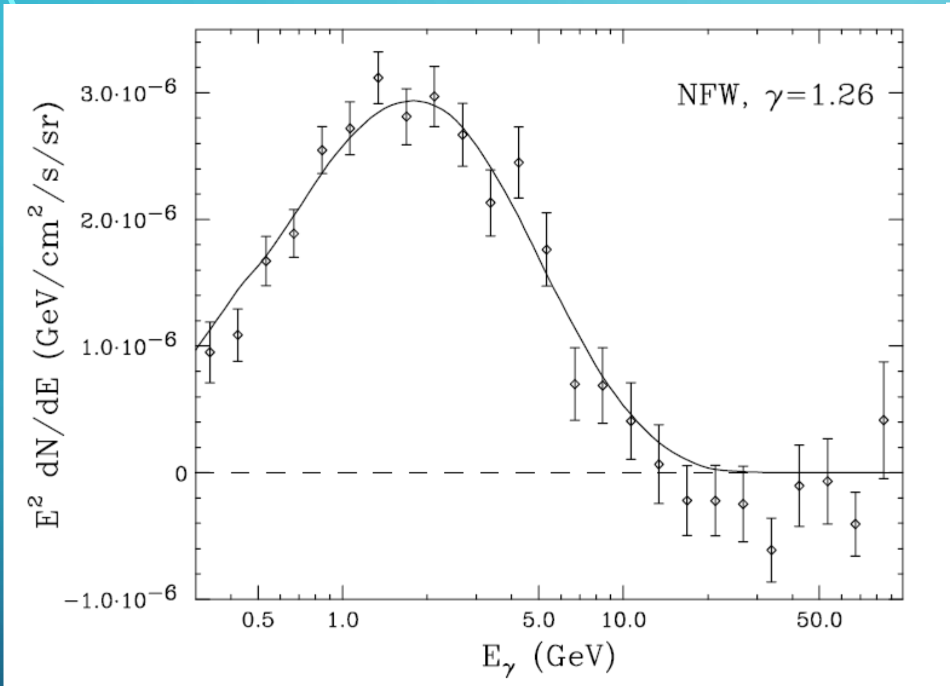

Daylan et al. 2015

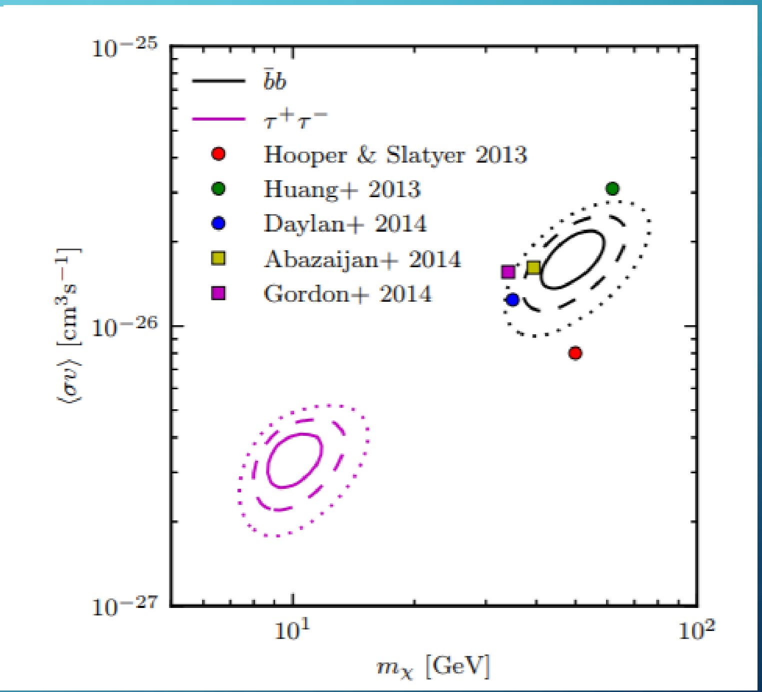

Calore et al. 2015

PHYSICAL REVIEW D **91,** 123010 (2015)

GeV excess in the Milky Way: The role of diffuse galactic gamma-ray emission templates

Bei Zhou,[1,2] Yun-Feng Liang,[1,2] Xiaoyuan Huang,[1,*] Xiang Li,[1,2,†] Yi-Zhong Fan,[1,‡] Lei Feng,[1] and Jin Chang[1]

Diffuse Galactic γ-ray Emission: Models

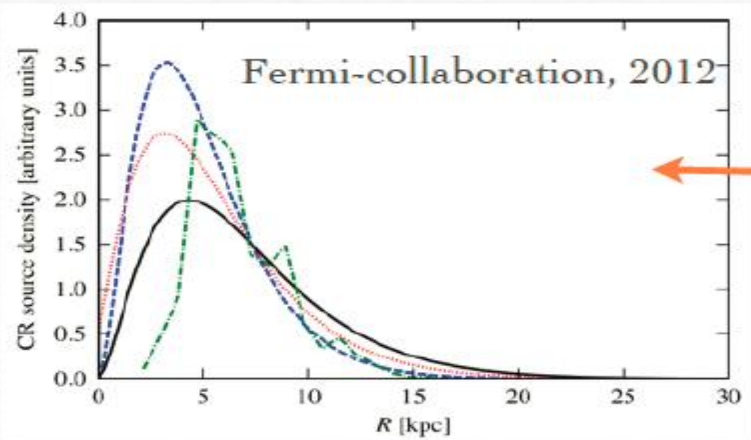

	Sources	Propagation		Targets	
Value	SS	ZZ	R	T	C
00	SNR	4 kpc	20 kpc	150 K	2 mag
01	Lorimer	6 kpc	30 kpc	Optically thin	5 mag
10	Yusifov	8 kpc			
11	OB stars	10 kpc			

Note. SS stands for CR s... for the $E(B-V)$ magni...

Fer...

$4 \times 4 \times 2 \times 2 \times 2 = 128$

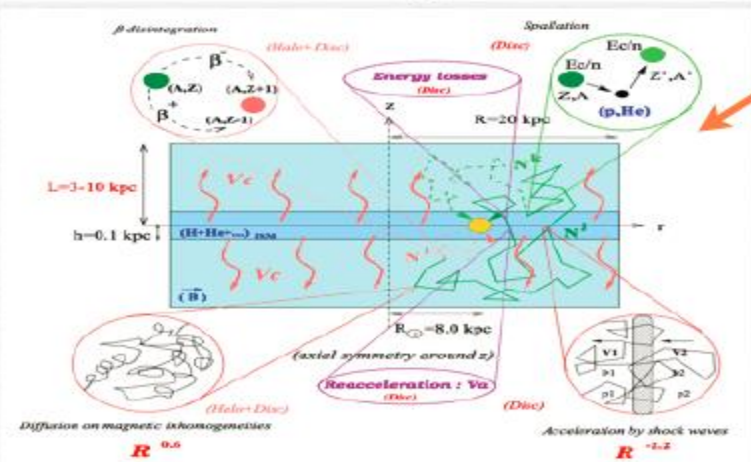

Maurin et al., 2002

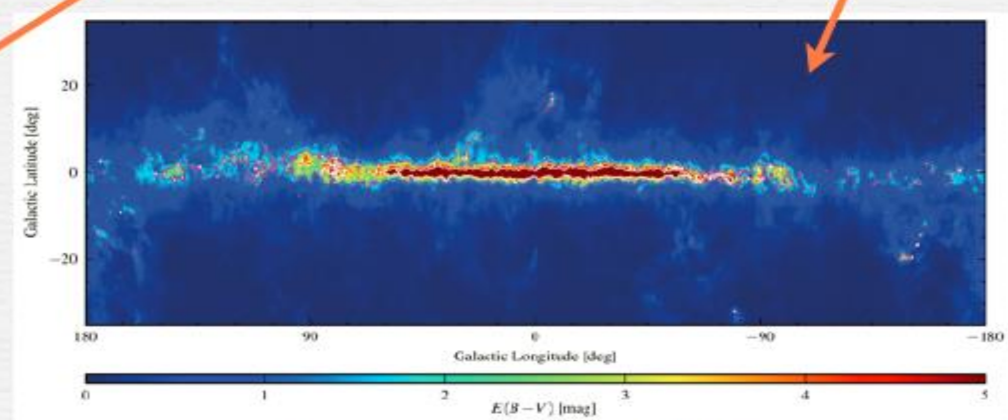

Fermi-collaboration, 2012

The template dependence of GEV excess signal

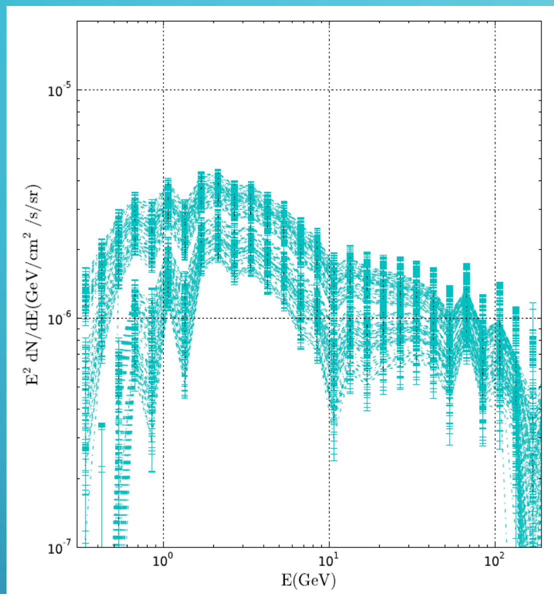

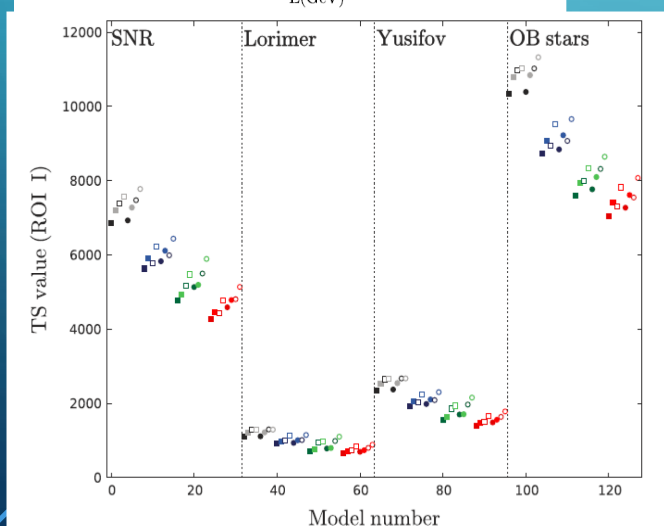

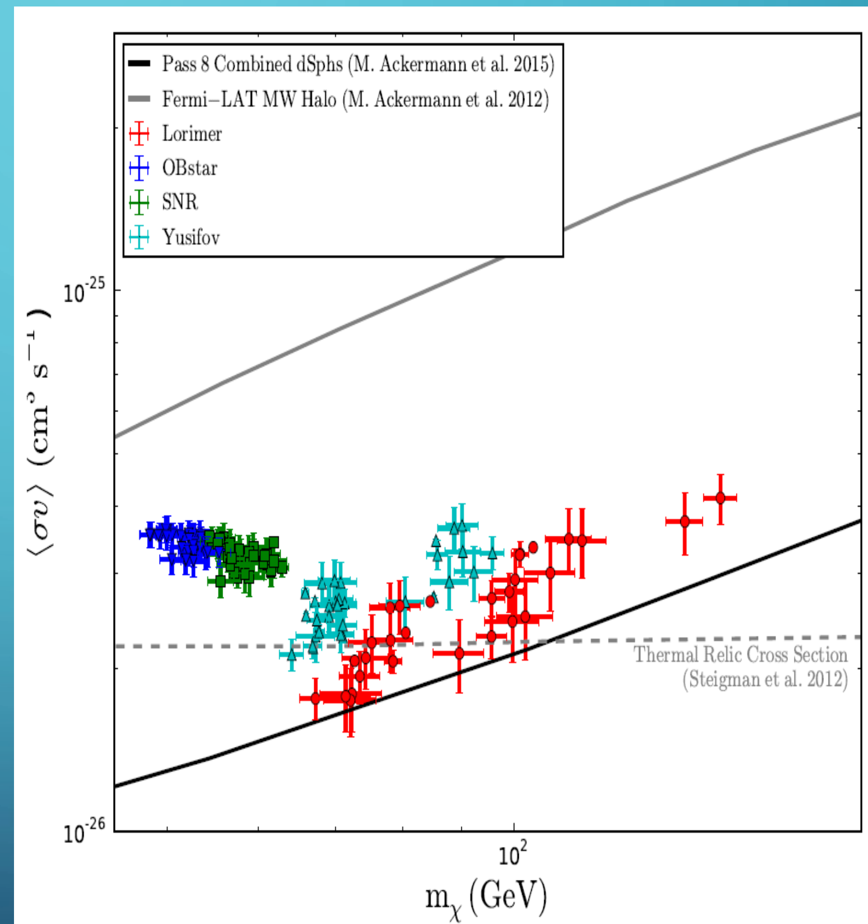

GEV EXCESS IN THE DWARF GALAXIES?

TABLE I: DES2 dSph Candidates and the Estimated J-factors

Name	(l,b)[a] (deg)	Distance[b] (kpc)	$\log_{10}$ (Est.J)[c] $\log 10(\mathrm{GeV}^2\mathrm{cm}^{-5})$
DES J2204-4626	(351.15,-51.94)	53 ± 5	18.8
DES J2356-5935	(315.38,-56.19)	25 ± 2	19.5
DES J0531-2801	(231.62,-28.88)	182 ± 18	17.8
DES J0002-6051	(313.29,-55.29)	48 ± 4	18.9
DES J0345-6026	(273.88,-45.65)	92 ± 13	18.3
DES J2337-6316	(316.31,-51.89)	55 ± 9	18.8
DES J2038-4609	(353.99,-37.40)	214 ± 16	17.6
DES J0117-1725	(156.48,-78.53)	30 ± 3	19.3

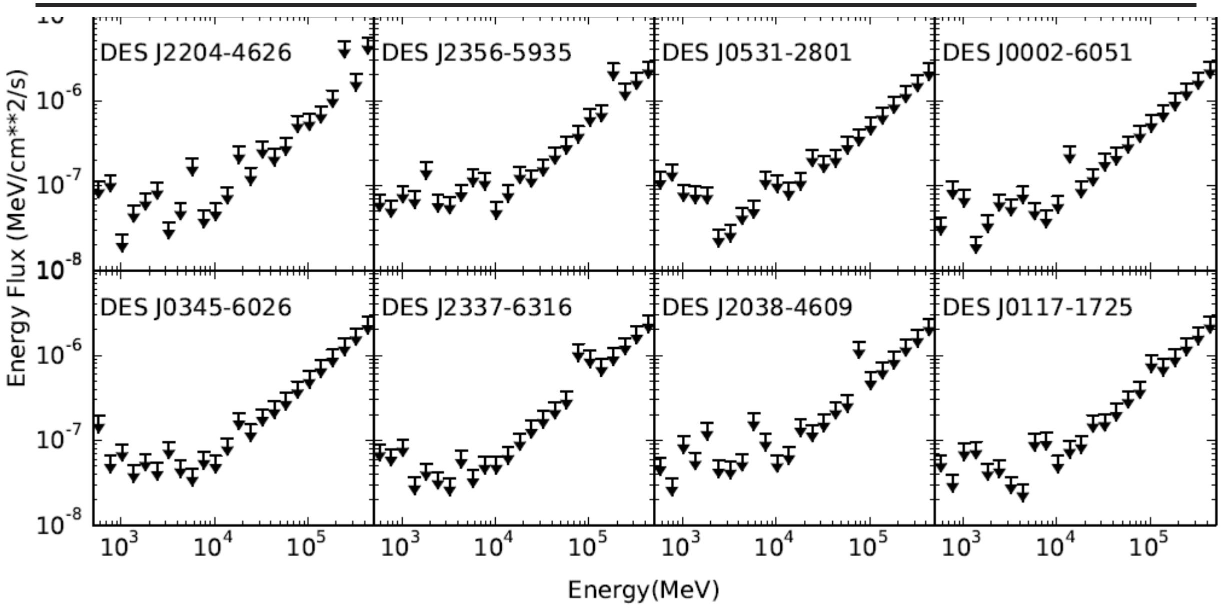

Shang Li et al PRD 2016

GeV Excess in the Dwarf Galaxies?

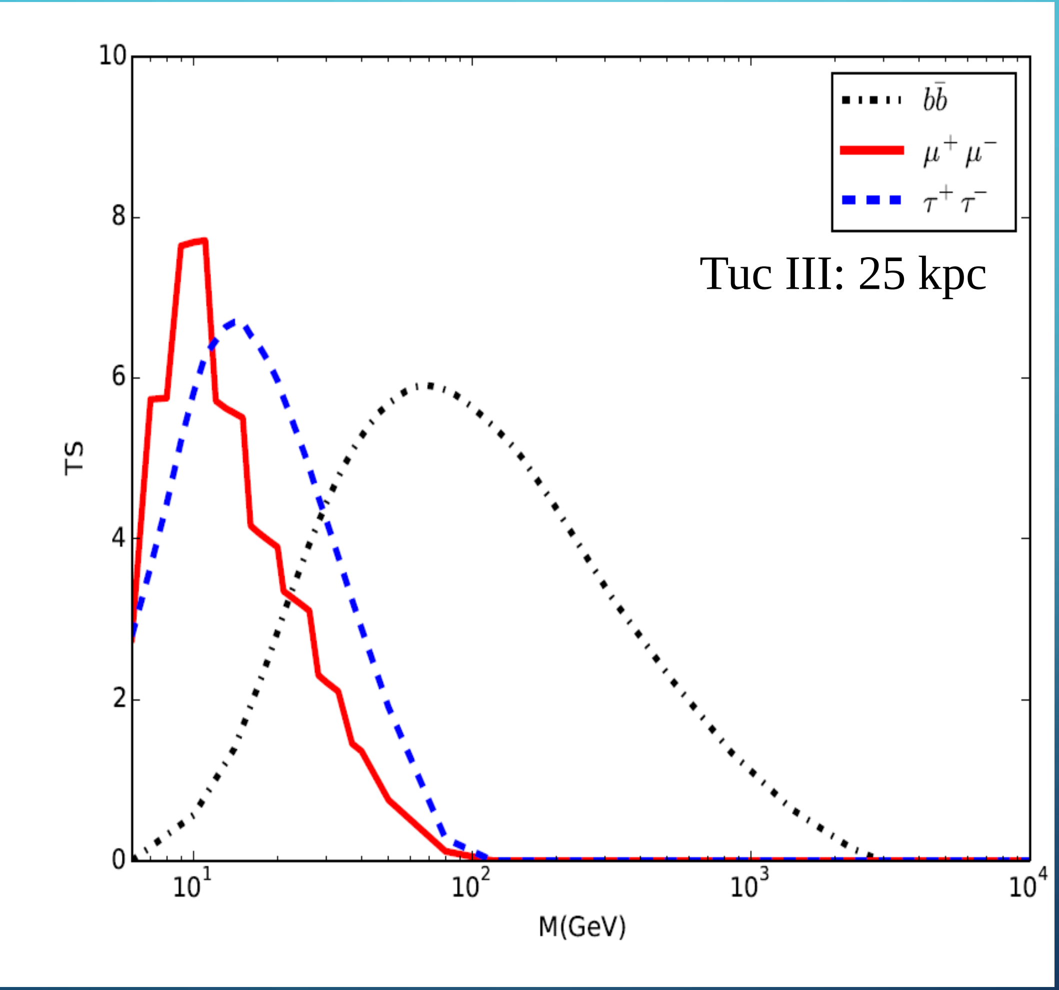

Li, S. et al. PRD (2016)

Evidence for Gamma-ray Emission from the Newly Discovered Dwarf Galaxy Reticulum 2

Alex Geringer-Sameth[*] and Matthew G. Walker[†]
McWilliams Center for Cosmology, Department of Physics, Carnegie Mellon University, Pittsburgh, PA 15213, USA

Savvas M. Koushiappas[‡]
Department of Physics, Brown University, Providence, RI 02912, USA

Sergey E. Koposov, Vasily Belokurov, Gabriel Torrealba, and N. Wyn Evans
Institute of Astronomy, University of Cambridge, Cambridge, CB3 0HA, UK
(Dated: March 10, 2015)

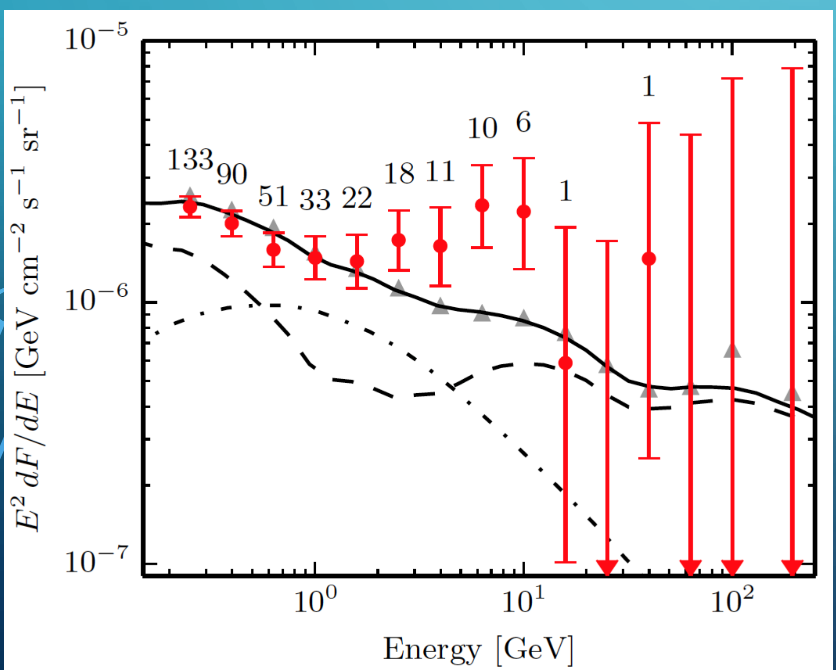

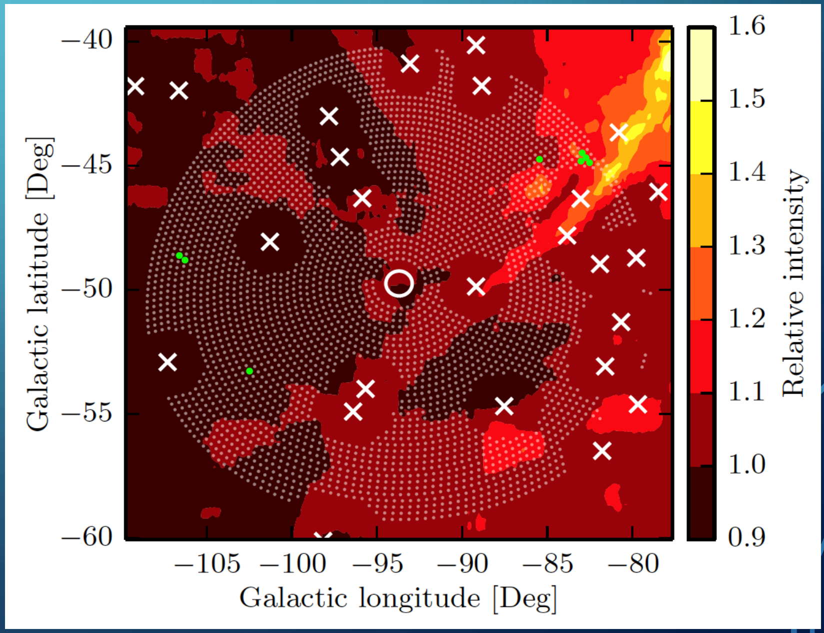

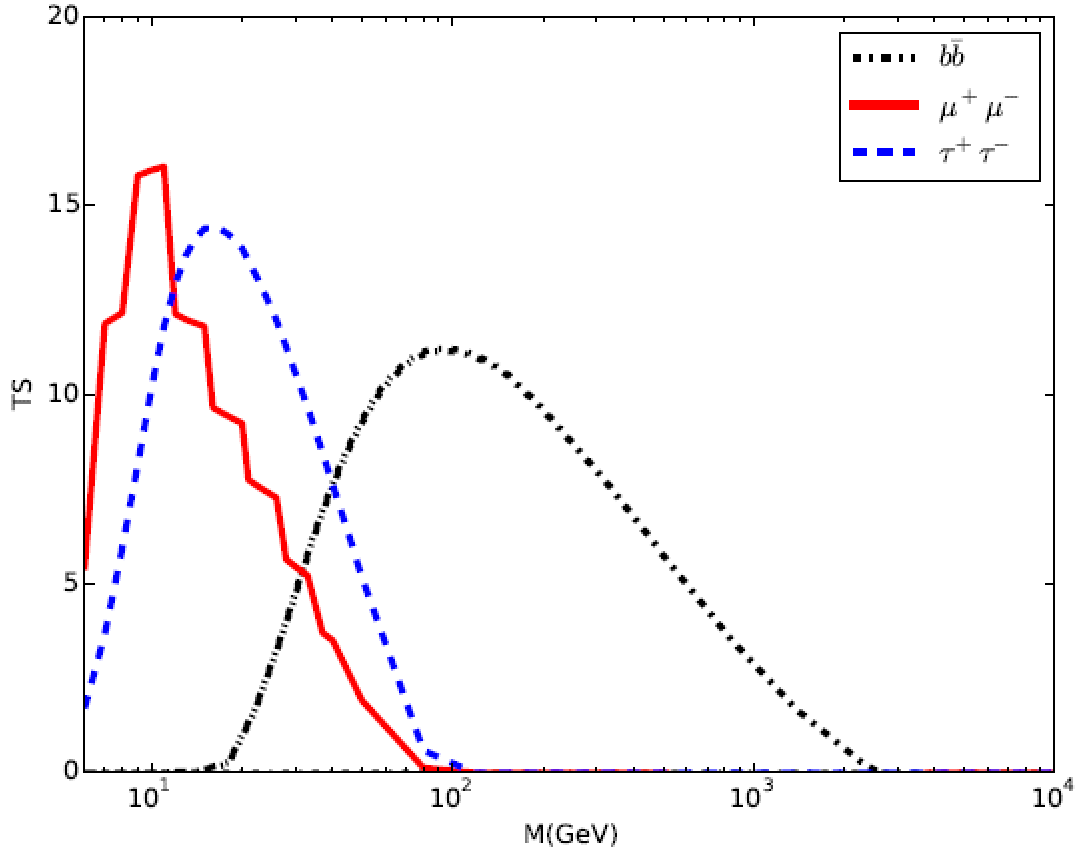

FIG. 4: The TS value of the possible dark matter annihilation signal in the combined γ−ray data in the directions of both Ret II and Tuc III. The dark matter annihilation channels are labeled in the plot.

SEARCH FOR A GAMMA-RAY LINE FEATURE FROM A GROUP OF NEARBY GALAXY CLUSTERS

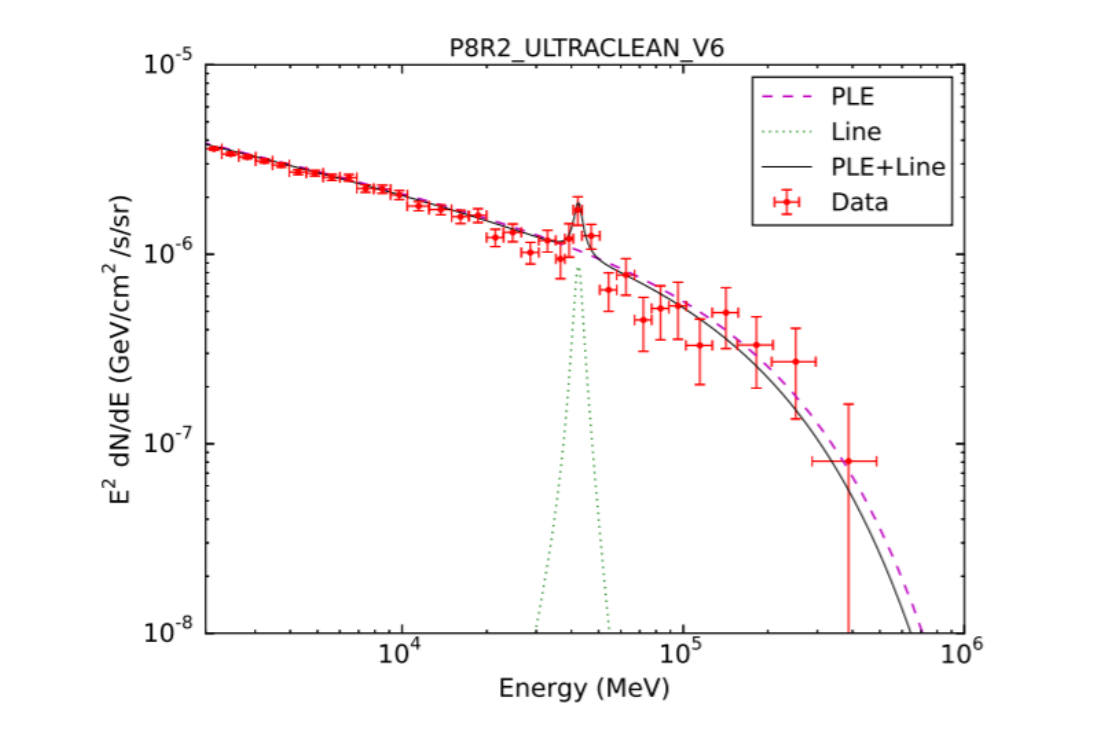

Yun-Feng Liang et al., Phys.Rev. D93 (2016) no.10, 103525

GAMMA RAY LINE DETECTED BY DAMPE

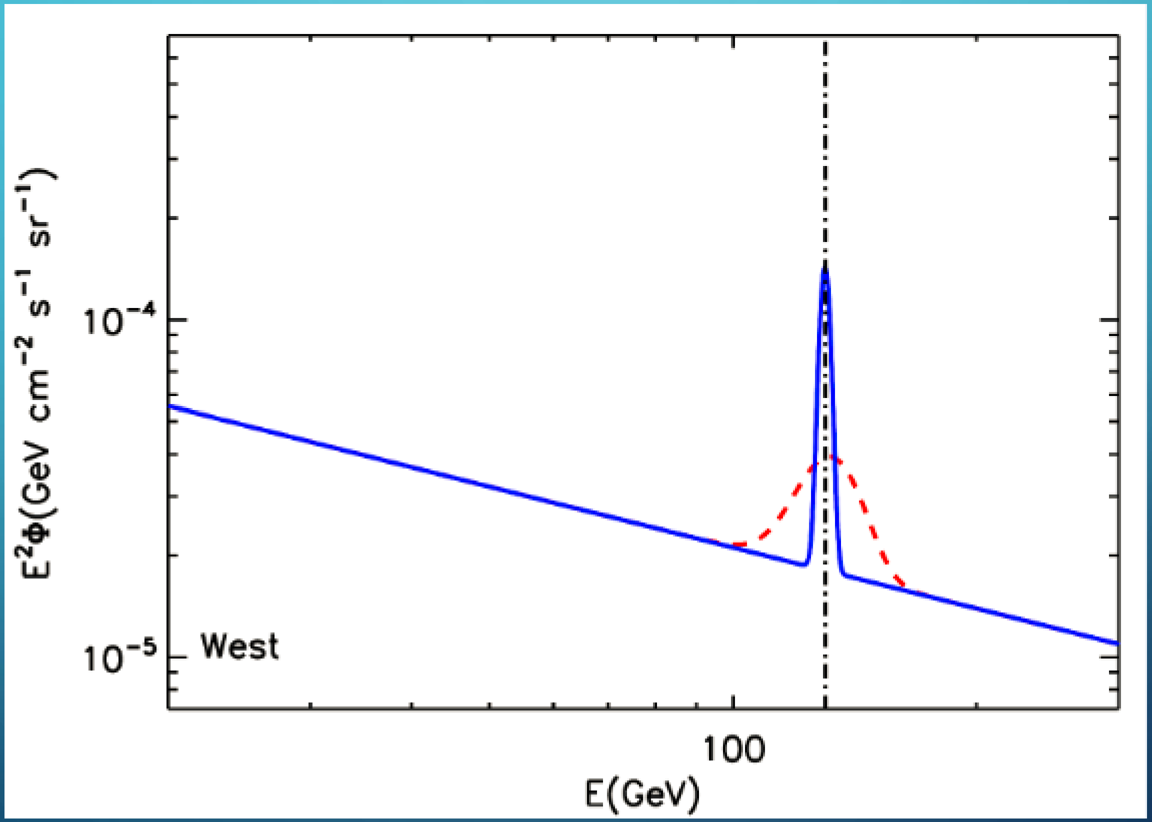

Ye Li and Qiang Yuan PLB (2015)

OUTLINE

- What is Axion and ALP？
- Dark matter and DM searching in gamma ray data
- Searching ALP in gamma ray data and Our works

EXPLORE AXION AND ALP IN GAMMA RAY DATA

- Primakoff Process :

  Axions and ALPs can convert to photons and vice versa in electromagnetic fields

- As for axion, the axion mass is proportional to the coupling. For ALPs, they are mutually independent.

$$\mathcal{L} = g_{a\gamma}\vec{E}\cdot\vec{B}a,$$

the coupling

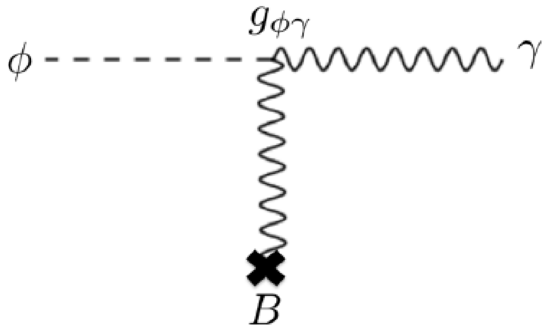

LIGHT SHINING IN BLACK BOX

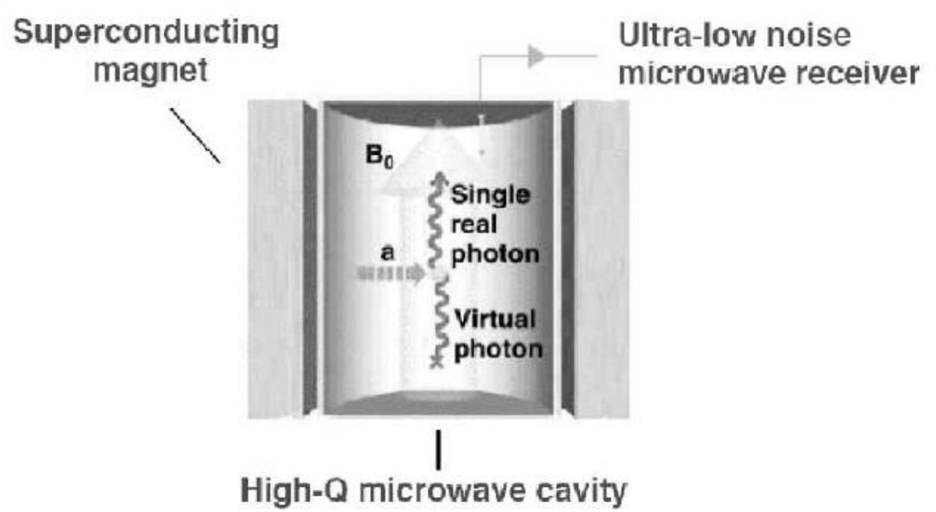

Fig. 1. Schematic principle of the microwave cavity experiment to look for cold dark matter axions. First an axion would be resonantly converted into a quasi-

ADMX

SOLAR AXIONS SEARCHES

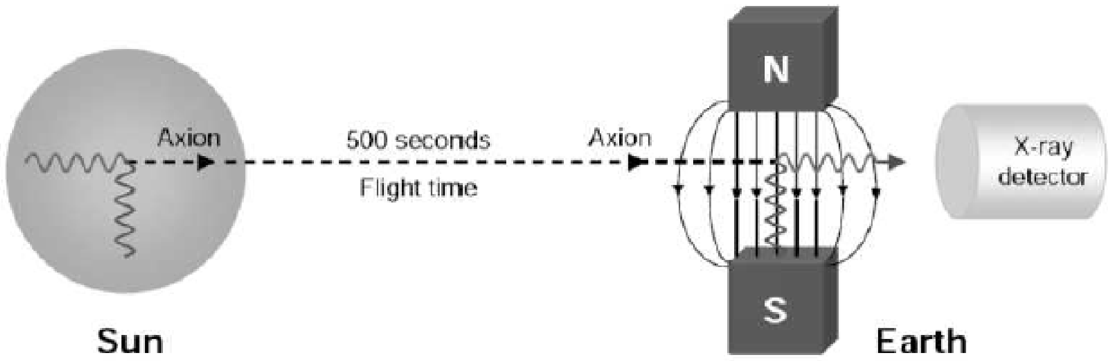

Fig. 4. Working principle of an axion helioscope. Axions produced in the Sun core by the Primakoff effect would be converted back into photons in a strong magnetic field. Eventually these photons, which have the same energy spectrum as the incoming axions, could be collected by a X-ray detector placed a the end of the magnet field area

CAST

GEOMAGNETIC AXION CONVERSION

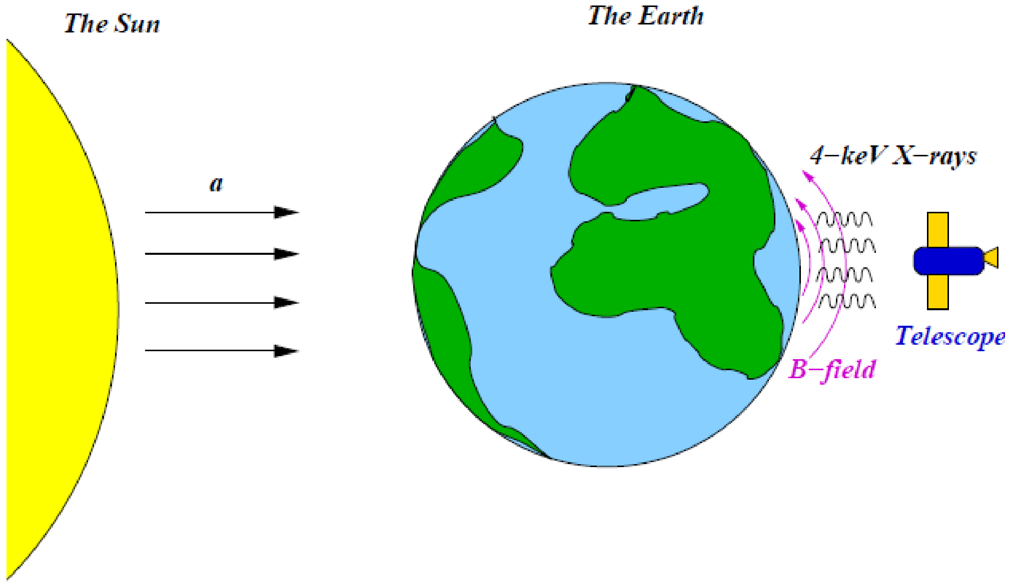

Fig. 7. The observational setup to detect geomagnetic converted axions (GECOSAX). The Sun is used as an axion source and a satellite based X-ray observatory to detect the photons from geomagnetically converted axions. The Earth acts as a shield for direct X-rays coming from the Sun and other X-ray sources on the sky

LIGHT SHINING THROUGH A WALL

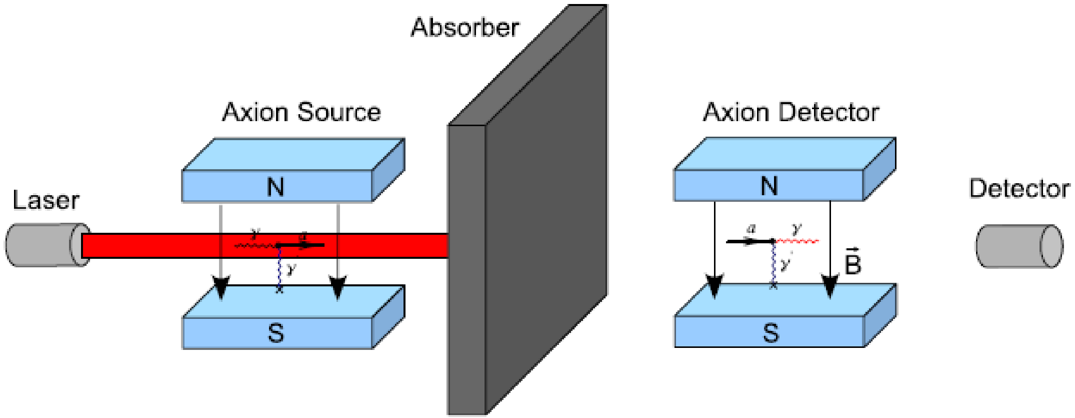

Fig. 10. Schematic view of a photon regeneration or light shining through a wall experiment. A polarized laser beam enters a transverse magnetic field from the left.

The pioneering experiment based on this technique was performed by the Brookhaven-Fermilab-Rutherford-Trieste (BFRT) collaboration.

EXPLORE AXION AND ALP IN GAMMA RAY DATA

THE SURVIVAL PROBABILITY

$$P_{\rm osc} = \sin^2(2\theta)\,\sin^2\left[\frac{g_{a\gamma}\,B\,s}{2}\sqrt{1+\left(\frac{\mathcal{E}}{E_\gamma}\right)^2}\,\right], \qquad (3)$$

where s is the size of the domain and B is the magnetic field component along the polarization vector of the photon, which is assumed to be approximately constant within that domain. We have also defined an effective mixing angle θ and characteristic energy $\mathcal{E}$ via

$$\sin^2(2\theta) = \frac{1}{1+(\mathcal{E}/E_\gamma)^2}\,, \qquad \mathcal{E} \equiv \frac{m^2}{2g_{a\gamma}\,B}\,, \qquad (4)$$

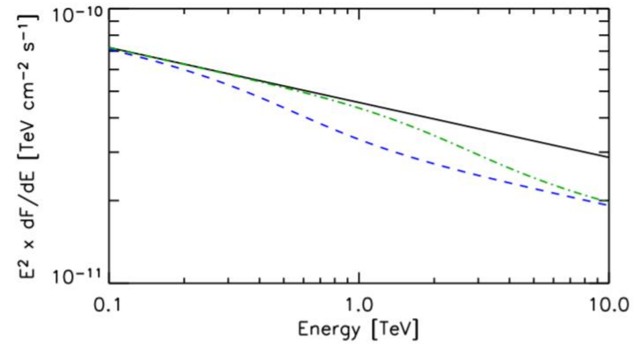

FIG. 1: A typical power-law γ-ray spectrum (solid line) and its distortion for photon-ALP conversion with $\mathcal{A} = 1/3$ and critical energies $\mathcal{E} = 500$ GeV (dashed lines) and $\mathcal{E} = 2.5$ TeV (dashed-dotted line). See text for details.

Hooper, Dan *et al.* Phys.Rev.Lett. 99 (2007) 231102 arXiv:0706.3203

HOW TO CALCULATION THE THE SURVIVAL PROBABILITY

Von-Neumann-like commutator equation, e.g. [69],

$$i\frac{\mathrm{d}\rho}{\mathrm{d}x_3} = [\rho, \mathcal{M}]\,, \tag{3}$$

with the mixing matrix $\mathcal{M}$. The photon-ALP mixing is induced by the transversal magnetic field $\mathbf{B}_\perp$ only. For a homogenous field orientated along x_2, $\mathbf{B}_\perp = B\hat{\mathbf{e}}_2$, the mixing matrix reads [12, 70],

$$\mathcal{M} = \begin{pmatrix} \Delta_\perp & 0 & 0 \\ 0 & \Delta_{||} & \Delta_{a\gamma} \\ 0 & \Delta_{a\gamma} & \Delta_a \end{pmatrix}, \tag{4}$$

$$\Delta_{||} \equiv \Delta_{\rm pl} + 3.5\,\Delta_{\rm QED}\,, \tag{10}$$

$$\Delta_\perp \equiv \Delta_{\rm pl} + 2\,\Delta_{\rm QED}\,, \tag{11}$$

$$\Delta_{a\gamma} \equiv \frac{1}{2} g_{a\gamma} B_T \simeq 1.52\times 10^{-2}\left(\frac{g_{a\gamma}}{10^{-11}\,\mathrm{GeV}^{-1}}\right)\left(\frac{B_T}{10^{-9}\,\mathrm{G}}\right)\mathrm{Mpc}^{-1}\,, \tag{12}$$

$$\Delta_a \equiv -\frac{m^2}{2E} \simeq -7.8\times 10^{-3}\left(\frac{m}{10^{-13}\,\mathrm{eV}}\right)^2\left(\frac{E}{10^2\,\mathrm{keV}}\right)^{-1}\mathrm{Mpc}^{-1}\,, \tag{13}$$

with

$$\Delta_{\rm pl} \equiv -\frac{\omega_{\rm pl}^2}{2E} \simeq -1.1\times 10^{-4}\left(\frac{E}{10^2\,\mathrm{keV}}\right)^{-1}\left(\frac{n_e}{10^{-7}\,\mathrm{cm}^{-3}}\right)\mathrm{Mpc}^{-1}\,, \tag{14}$$

$$\Delta_{\rm QED} \equiv \frac{\alpha E}{45\pi}\left(\frac{B_T}{B_{\rm cr}}\right)^2 \simeq 4.1\times 10^{-16}\left(\frac{E}{10^2\,\mathrm{keV}}\right)\left(\frac{B_T}{10^{-9}\,\mathrm{G}}\right)^2\mathrm{Mpc}^{-1}\,, \tag{15}$$

Equation (3) is solved by means of the transfer matrix $\mathcal{T}$, $\rho(x_3) = \mathcal{T}(x_3, 0; E)\rho(0)\mathcal{T}^\dagger(x_3, 0; E)$, with the initial condition $\mathcal{T}(0, 0; E) = 1$, e.g. [17, 23, 38, 72]. Neither the magnetic field in the Perseus cluster nor the Galactic magnetic field are homogeneous. Therefore, the path in the different B fields is split up into N segments. In each segment, $\mathbf{B}_\perp$ is assumed to be constant and forms an angle ψ_i, $(i = 1, \ldots, N)$ with the x_2 axis. The B field is modeled as a a divergence-free homogeneous isotropic field with Gaussian turbulence [40] The full transfer matrix is then

$$\mathcal{T}(x_{3,N}, x_{3,1}; \psi_N, \ldots, \psi_1; E) = \prod_{i=1}^{N} \mathcal{T}(x_{3,i+1}, x_{3,i}; \psi_i; E). \qquad (5)$$

In this setup, the probability to observe a photon of either polarization $\rho_{jj} = \mathrm{diag}(\delta_{1j}, \delta_{2j}, 0)$ after the N-th domain is given by

$$P_{\gamma\gamma} = \sum_{j=1,2} \mathrm{Tr}\left(\rho_{jj}\mathcal{T}\rho_0\mathcal{T}^\dagger\right). \qquad (6)$$

REAL MAGNETIC FIELD SITUATION

Intra-cluster magnetic field

Faraday RM observations and magneto-hydrodynamic simulations suggest that the magnetic field in galaxy clusters is turbulent and that its strength follows the electron density $n_e(r)$ of the intra-cluster medium (ICM), $B(r) = B_0(n_e(r)/n_e(r=0))^\eta$ [46–48]. We model the turbulent component as a divergence-free homogeneous isotropic field with Gaussian turbulence with zero mean and a variance σ_B [40]. The energy density follows a

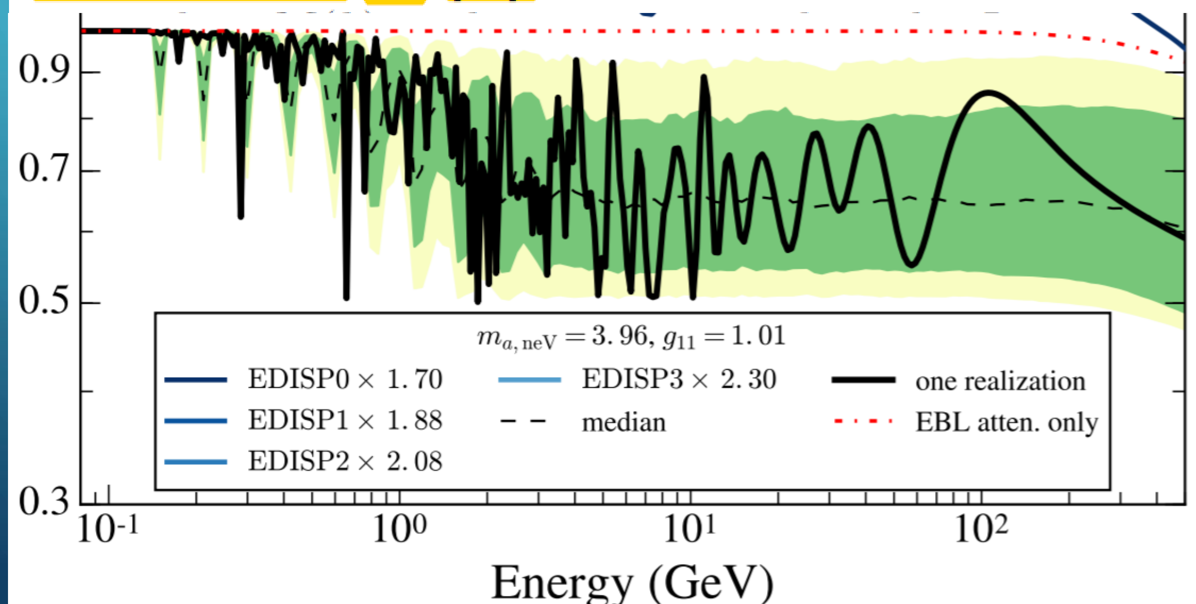

THE GAMMA RAY DATA IN ALP MODEL

Under the ALP hypothesis, characterized by $P_{\gamma\gamma} \equiv P_{\gamma\gamma}(E, m_a, g_{a\gamma}, \mathbf{B}_j)$ for one random turbulent B-field realization $\mathbf{B}_j$, the expected number of photons is calculated through

$$\mu_{ik'} = \sum_k \mathcal{D}^i_{kk'} \int_{\Delta E_k} dE \, P_{\gamma\gamma} F(E) \mathcal{E}^i(E), \qquad (2)$$

where the integration runs over the true energy bin ΔE_k, $\mathcal{E}^i$ is the exposure, and $\mathcal{D}^i_{kk'}$ is the energy dispersion for event type EDISPi. Under the null hypothesis, $P_{\gamma\gamma}$ reduces to the EBL attenuation. The parameters of the intrinsic source spectrum $F(E)$, N, α, and β, are further nuisance parameters. For each tested ALP parameter

Phys. Rev. Lett. 116, 161101 (2016).

Search for Spectral Irregularities due to Photon–Axionlike-Particle Oscillations with the Fermi Large Area Telescope

M. Ajello,[1] A. Albert,[2] B. Anderson,[3,4] L. Baldini,[5,2] G. Barbiellini,[6,7] D. Bastieri,[8,9] R. Bellazzini,[10]

We report on the search for spectral irregularities induced by oscillations between photons and axionlike-particles (ALPs) in the γ-ray spectrum of NGC 1275, the central galaxy of the Perseus cluster. Using six years of *Fermi* Large Area Telescope data, we find no evidence for ALPs and

For the turbulence spectrum, we assume values derived from RMs of the cool-core cluster A 2199 [52], which has a comparable number of member galaxies. The fiducial parameter choices are summarized in Tab. I.

Parameter	Value
σ_B	$10\,\mu$G
r_{max}	500 kpc
η	0.5
q	-2.8
Λ_{min}	0.7 kpc
Λ_{max}	35 kpc

TABLE I. Fiducial model parameters for the intra-cluster magnetic field in Perseus.

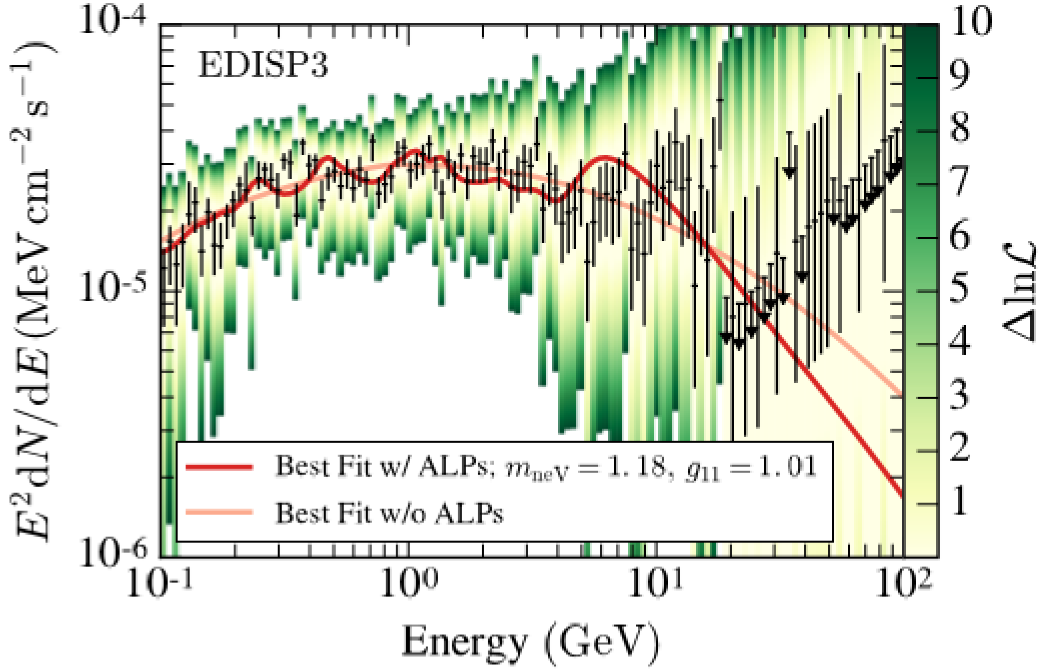

FIG. 1. The likelihood curves (shown in color) for the EDISP3 event type. $\Delta \ln \mathcal{L} = 0$ corresponds to the maximum likelihood in each bin (black points). The error bars indicate an increase of the likelihood by $2\Delta \ln \mathcal{L} = 1$. The best-fit spectrum of the joint likelihood without an ALP (with an ALP with $m_{\rm neV} = 1.2$ and $g_{11} = 1$) is shown as a light (dark) red solid line.

THE RESULT

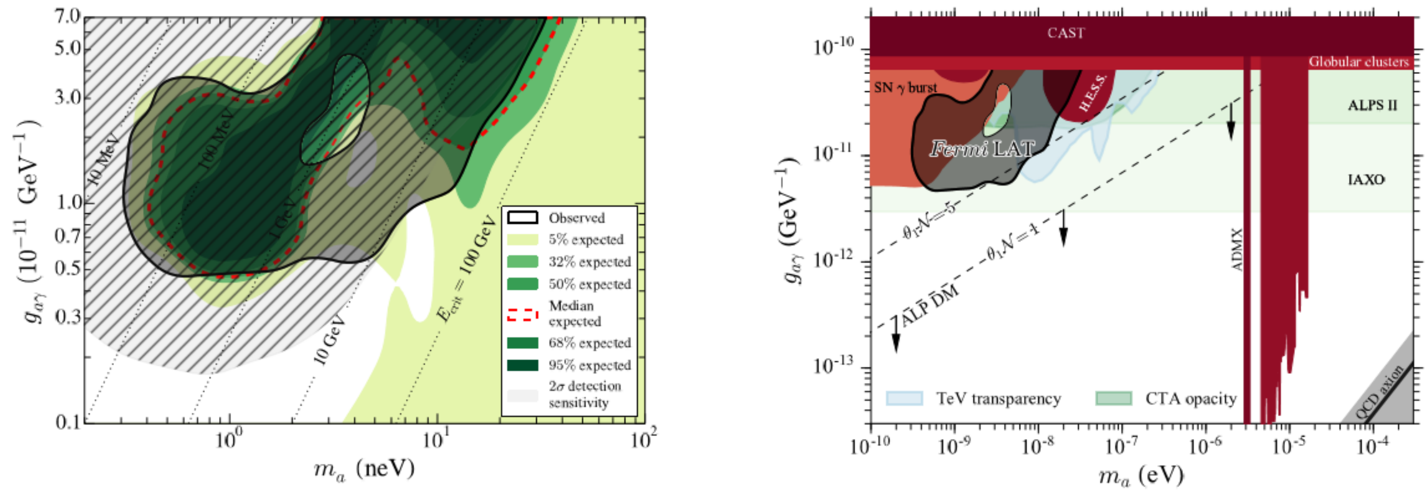

FIG. 2. *Left*: Observed and expected 95 % confidence limits on the ALP parameters from 400 Monte-Carlo simulations. Dotted lines correspond to constant critical energies. The hatched gray region shows the parameters where ALPs are detectable at the 2σ confidence level (median sensitivity). *Right*: Comparison of *Fermi*-LAT limits with other works. Other Limits are shown in red, expected sensitivities in green. The parameter space where ALPs could explain a low γ-ray opacity is shown in blue. ALPs below the $\mathcal{N}\theta_1 = 1$ line could account for all the DM. The QCD axion is shown as a gray shaded band and solid black line. See, e.g. [67] and references therein.

OUR WORK (I)

- Searching the ALP signal from the Fermi LAT data in BL Lac object PKS 2155−304 (z=0.116)
- Similar method was used as in Phys. Rev. Lett.116, 161101

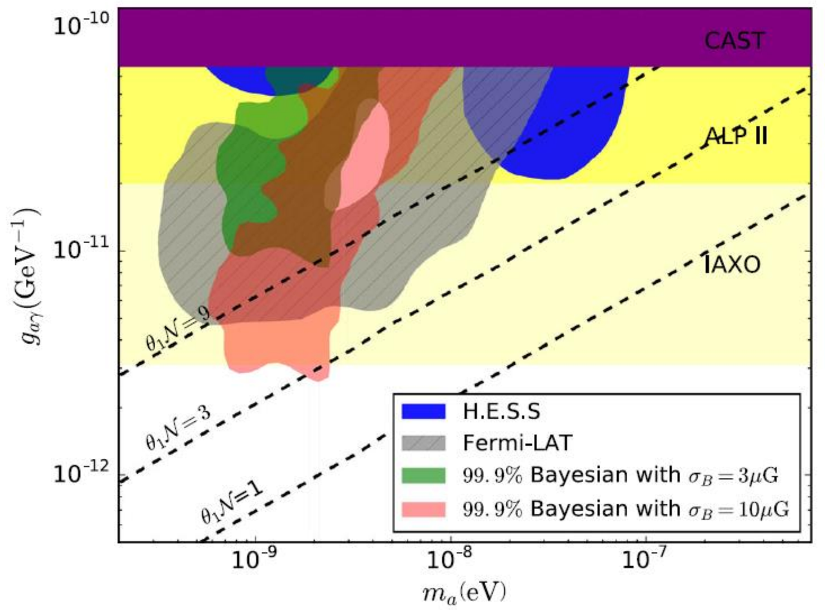

FIG. 2. Exclusion regions (green for $\sigma_B = 3\ \mu G$ and red for $\sigma_B = 10\ \mu G$) of the ALP parameter space (m_a, $g_{a\gamma}$) at 99.9% credible level derived in this work, compared with those obtained by Fermi-LAT observation of NGC 1275 (gray [1]) and H.E.S.S.

Cun Zhang, Yun-Feng Liang, Shang Li, Neng-Hui Liao, Lei Feng, Qiang Yuan, Yi-Zhong Fan, Zhong-Zhou Ren, Phys.Rev. D97 (2018) no.6, 063009

OUR WORK (II)

- Searching for spectral oscillations due to photon-ALP conversion using the Fermi-LAT observations of bright supernova remnants

- Data Analyses：

  Calculate **survival probabilities for photons** from SNRs. Perform **the Chi-Square analysis** on the Fermi-LAT spectra for the models with or without the photon-ALP oscillation separately.

Name	lon [°]	lat [°]	d [kpc]	$TS_{Bfield1}$	$TS_{Bfield2}$	$TS_{Bfield3}$
IC443	189.065	3.235	1.5	21.2	21.5	21.8
W44	6.660	-0.180	1.9	4.7	3.4	3.2
W51C	49.131	-0.467	5.5	2.2	3.1	5.0

OUR WORK (II)

Zi-Qing Xia, Cun Zhang, Yun-Feng Liang, Lei Feng, Qiang Yuan, Yi-Zhong Fan, Jian Wu. Phys.Rev. D97 (2018) no.6, 063003

IC443: Show an intriguing indication of photon-ALP mixing?

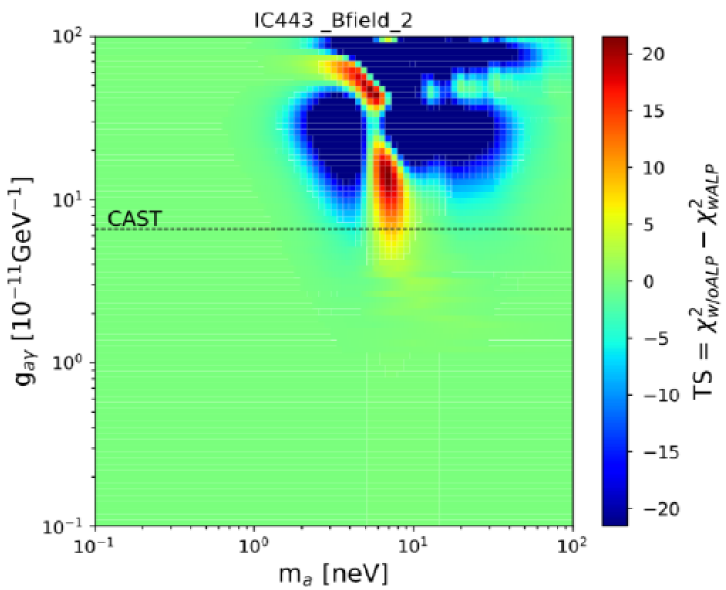

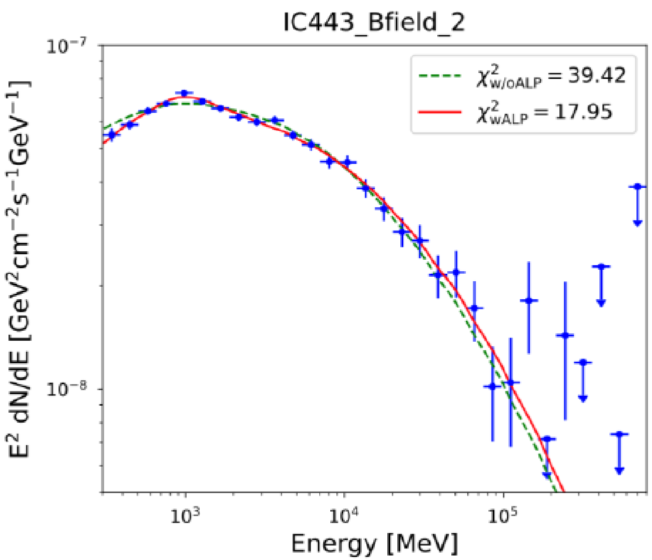

The best-fit parameters is excluded by the CAST experiment.

OUR WORK (III)

- Constraints on ALP properties with H.E.S.S. observations of Galactic gamma-ray sources

- Samples: Some bright sources located in the Galactic plane

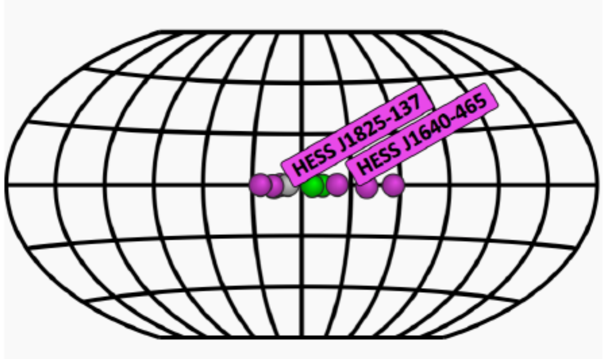

Name	Distance	Gal Lat	Gal Lon
RX J1713.7-3946	1.0 kpc	-0.4726856243282...	347.335519025031
LS 5039	2.5 kpc	-1.27810570904673	16.9021857350709
HESS J1731-347	3.2 kpc	-0.6698	353.5424
HESS J1825-137	3.9 kpc	-0.6968714372208...	17.7106538603428
HESS J1813-178	4.7 kpc	-0.0262889491377...	12.8115067285094
MSH 15-52	5.2 kpc	-1.19304386512435	320.330329434916
HESS J1804-216	6.0 kpc	-0.0284	8.4002
HESS J1303-631	6.6 kpc	-0.3340222360313...	304.213243514506
HESS J1837-069	6.6 kpc	-0.1157232713989...	25.1775852624532
HESS J1640-465	8.6 kpc	-0.0185900990789...	338.317160821871

OUR WORK (III)

HESSJ1640-465 D=8.6kpc

Red regions are excluded.

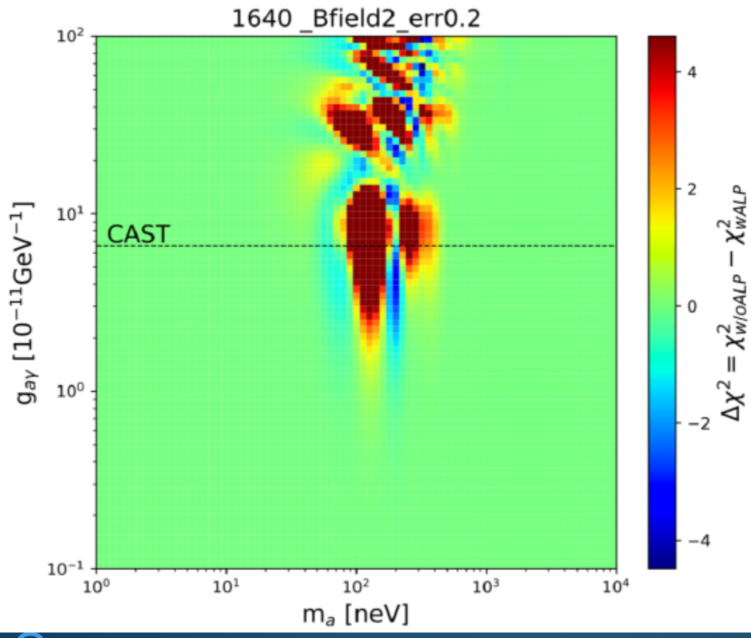

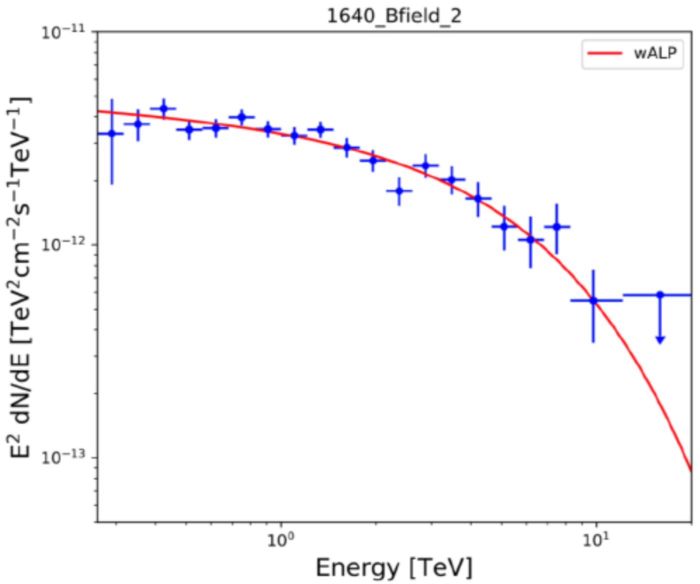

OUR WORK (III)

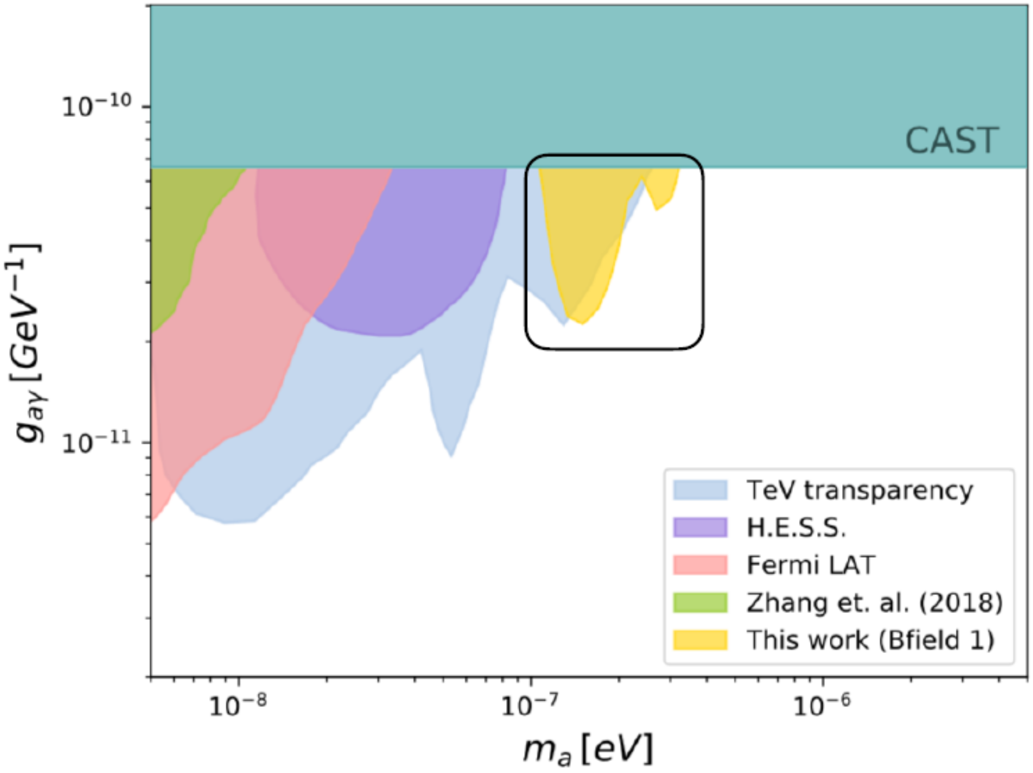

A part of the parameter space explaining the low γ-ray opacity of the universe can be excluded by the H.E.S.S. observations.

SYSTEMATIC UNCERTAINTIES

- Galactic magnetic field model (using three different model)
- Energy binning
- The detector's energy resolution and effective area

CONCLUSIONS

- No confirm ALP signals was found in gamma ray data
- Lots of tight constrains were obtained
- Best energy resolution is important and DAMPE is helpful.

DISCUSSIONS

- Constrains with optical data?
- Constrains with X-ray data?
- Combine the data of different band for one single source?
- Other possible target?


THE END
THANK YOU